THERMOMECHANICAL AND DEGRADATION BEHAVIOR OF BIO-BASED MATRIX NANOCOMPOSITES

P. Georgiopoulos[a] , E. Kontou[a*], A. Meristoudi[b], S. Pispas[b]

[a] *School of Applied Mathematical and Physical Sciences*
Department of Mechanics, National Technical University of Athens
5 Heroes of Polytechnion, 15773, Athens, Greece
[b] *Theoretical and Physical Chemistry Institute, National Hellenic Research Foundation,*
48 Vass. Constantinou Ave., 11635, Athens, Greece
** ekontou@central.ntua.gr*

Keywords: biodegradation, nanocomposites, thermomechanical properties

Abstract
The thermomechanical properties of a biodegradable polymer matrix, namely Poly(lactic Acid) (PLA) and its nanocomposites, based on silica nanoparticles are extensively studied. Scanning Electron Microscopy (SEM), Differential Scanning Calorimetry (DSC), and tensile testing are employed for the materials characterization. The degradation process of PLA and its nanocomposites under hydrolytic degradation at specific conditions, simulating the conditions into the human body has also been examined, in terms of Size Exclusion Chromatography (SEC) and Thermogravimetric Analysis (TGA).

1. Introduction

Polylactic acid (PLA) is nowadays one of the most important polymers, due to its combined properties, as biocompatibility, biodegradability, and adequate mechanical performance, appropriate for a wide range of medical, textile and packaging applications. PLA degrades during thermal processing or under hydrolytic conditions, giving a reduction of molecular weight that affects the final properties of the material, such as the mechanical strength [1]. The degradation behavior depends strongly on the molecular weight and the crystallinity of the PLA [2]. On the other hand, the thermomechanical and barrier properties of polylactide (PLA) can be enhanced by the incorporation of a fairly low amount of nanosized fillers (1-5 wt %) [3]. Many studies have been reported for a wide range of PLA nanocomposites [4]. In the present work, a series of PLA nanocomposites with a filler content of 2, 3 and 5 wt.% of silica (Si) has been prepared, and experimentally examined. The increment of the elastic modulus of PLA/Si nanocomposites with increasing nanofiller content was simulated with a micromechanical model developed in previous works. Considering that the nanoparticles generally take the form of agglomerates, a representative volume element (RVE) is consisted by a number of 'effective particles' with varying size, where agglomerates and the surrounding interphase region are also accounted for. The variation of the size of the dispersed phase is assumed to be expressed by a normal distribution function. The simulation of the experimental data of the tensile modulus lead to the estimation of an average value of interphase thickness over particle radius. A finite element analysis has also been performed, and compared to the analytical calculations. Besides the thermomechanical properties, the hydrolytic degradation behavior of PLA is also greatly affected by the presence of nanofillers.

The manner in which the thermomechanical properties of PLA and PLA/nanocomposites alter over time is still an issue of great importance. The degradation ability of PLA and PLA/Si nanocomposites under specific environmental conditions, namely immersion at a buffer solution at temperatures of 37 ˚C with a pH of 7.4 has been studied experimentally. These conditions simulate those in the human body, appropriate in medical applications. The majority of prior art studies on the stability of PLA have been carried out at similar physiological conditions [5], but there are still some issues that need to be addressed, such as the mechanical properties variation with aging time. Moreover, as it is mentioned in [6] the effect of silica on the hydrolytic degradation behavior of PLA is less researched. A matter of importance has been proved to be the crystallization behavior in PLA and the way it is affected by the presence of nanofillers during degradation procedure.

2. Experimental Results

2.1 . Differential Scanning Calorimetry (DSC) results

The DSC results of PLA and PLA/Si nanocomposites, as well as their variation with aging time, are shown in Table I. The Tg is generally increased with aging time for PLA and PLA/Si nanocomposites, with this increment being more essential in PLA matrix.

Material/ aging days	**T_g (ºC)**	**ΔH_m (J/g)**	**X_C (%)**	**T_m (ºC) T_{m1}/T_{m2}**	**Young's Modulus (GPa)**	**Yield stress (MPa)**
PLA						
0	58.42	22	18.0	154.4(146.1)	3.5	54.9
24	56.8	22.49	15.4	154.52(146.25)	3.0	52.65
86	57.1	23.77	18.1	155.2 (146)	3.03	54.4
125	58.4	24.66	16.8	155.8(146)	3.3	54.3
163	60.24	22.45	14.0	157.8(146.8)	3.11	49.6
250	63.7	27.72	19.8	156.0(146.0)	-	
PLA/Si/2						
0	58.81	22.55	24.24	155.3(151)	4.87	56.2
24	59.29	24.18	26.0	155.29(149.7)	3.6	53.32
86	58.1	25.52	27.44	155.9(149.54)	3.6	54.3
125	58.15	27.33	29.38	156.4(149.56)	3.64	51.0
163	60.15	24.71	26.56	157.74 (150)	3.75	
250	59.0	31.55	33.92	156.81(149.47)	-	
PLA/Si/3						
0	58.22	21.89	23.53	155.3 (150)	4.83	59.0
24	61.0	24.64	26.49	154.8(150.38)	3.67	53.2
86	58.2	25.62	27.54	155.9(149.7)	3.78	54.35
125	58.82	26.39	28.37	156.5(150.1)	4.0	49.5
163	59.6	27.34	29.39	156.3(149.5)	3.7	37.2
250	62.4	30.1	32.36	156.54(150)	-	
PLA/Si/5						
0	58.15	20.88	22.45	155.8(150.3)	4.85	58.7
24	61.5	23.47	25.23	154.7(149.8)	3.58	55.9
86	57.9	23.72	25.5	156.12(150.38)	3.62	53.62
125	60.31	22.79	24.5	157.1(150.1)	3.65	47.2
163	59.8	27.63	29.7	156.19(150.8)	3.87	39.3
250	62.34	30.2	32.36	156.67(149.5)	-	

Table 1. DSC and tensile properties of PLA/nanocomposites, with varying aging time

As far as crystalline behavior of PLA and PLA/nanocomposites under aging conditions is concerned, it must be noted that for a semicrystalline polymer, the initial crystalline structure strongly affects the hydrolytic degradation of PLA [6]. Generally, hydrolytic degradation occurs first in the amorphous region. The percentage crystallinity X_c of PLA with increasing aging time exhibits a non-monotonic behavior, but generally has a tendency to increase up to a value of 10% (Table I). PLA/Si nanocomposites on the other hand, appear a monotonic increment of X_c with aging time, up to values of the order of 40-44%. This effect must be an indication that silica is an effective nucleating agent, promoting the crystallization of PLA matrix, during the hydrolytic degradation [6]. It has been reported that the increased heat of fusion (and therefore Xc increment) is attributed to plasticization of PLA by water molecules as well as by lactic oligomers that would give sufficient mobility to the polymer chains to organize and further crystallize [7]. This is the result of two competitive effects: The silica content leads to the increase of the hydrophilicity of the sample, which results in the damage of more crystalline structure during the hydrolytic degradation process. On the other hand, due to degradation, we have easier crystal formation, and the nucleation of new crystalline regions, where smaller chains are involved. Analyzing further the evolution of crystalline structure during aging, the sample obtained at various aging time periods were examined by DSC. From Figure 1, illustrating representatively PLA and PLA/Si/3, as far as the melting region is concerned, two endothermic peaks appear in all material types. In previous works, the first peak T_{m1} has been related to the fusion of imperfect crystallites, formed through the cold crystallization process, while the second melting peak T_{m2} can be related to the crystallites formed during the melt-recrystallization process [8]. The two melting peaks become more intense with aging time, while the corresponding peak temperature remains generally

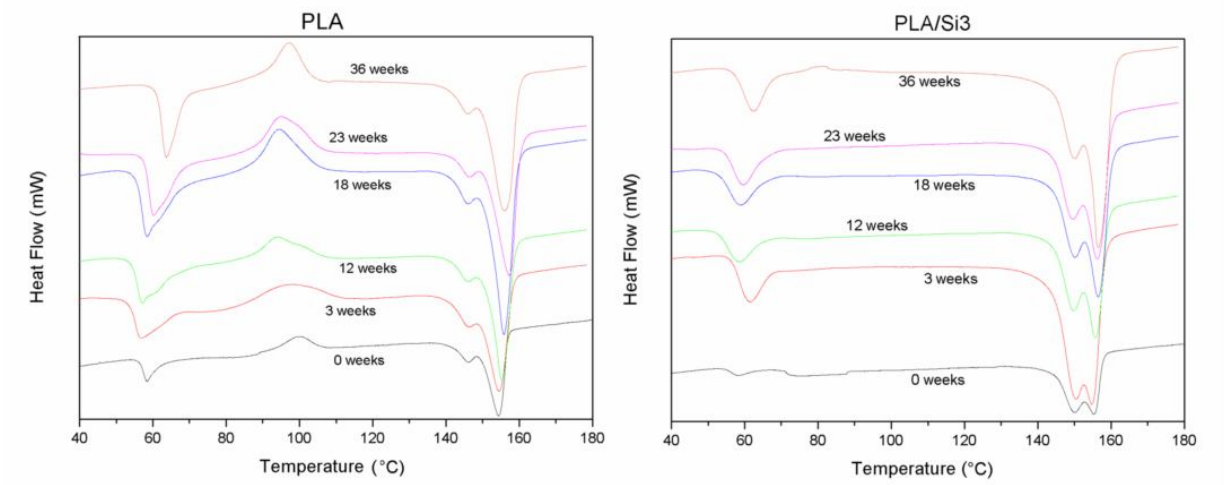

Figure 1. DSC curves of PLA and PLA/Si/3 at various aging times.

unaffected, or slightly increases. This fact combined with the enhancement of the total heat of fusion with aging, denotes that silica can promote the crystallization of PLA matrix during the hydrolytic degradation process, for the aging conditions applied.

2.2. Tensile testing results

The corresponding evolution of the tensile properties of pristine PLA and its nanocomposites with aging at the specific conditions examined, at various time periods are shown in Table I and Figure 2. From Table I, PLA/Si nanocomposites exhibit a 39% Young's modulus increment compared to the Young's modulus of PLA matrix. Following Table I, it can be

noticed that after 25 days of aging, PLA matrix undergoes a 14% reduction in the Young's modulus, while PLA/nanocomposites exhibit a 26% reduction. Hereafter, all studied samples exhibited almost the same trend in tensile properties during aging, that is the Young's modulus appears to be not further greatly affected, with increasing aging time. Finally, after 250 days of aging, the Young's modulus reduction for PLA is about 11%, while it is about 23% for PLA/nanocomposites. Therefore, it can be extracted that silica enhances degradability of PLA, while this enhancement slows down with increasing aging time, probably due to the crystallinity increment for PLA/nanocomposites. Similar trend is obtained for the yield stress variation.

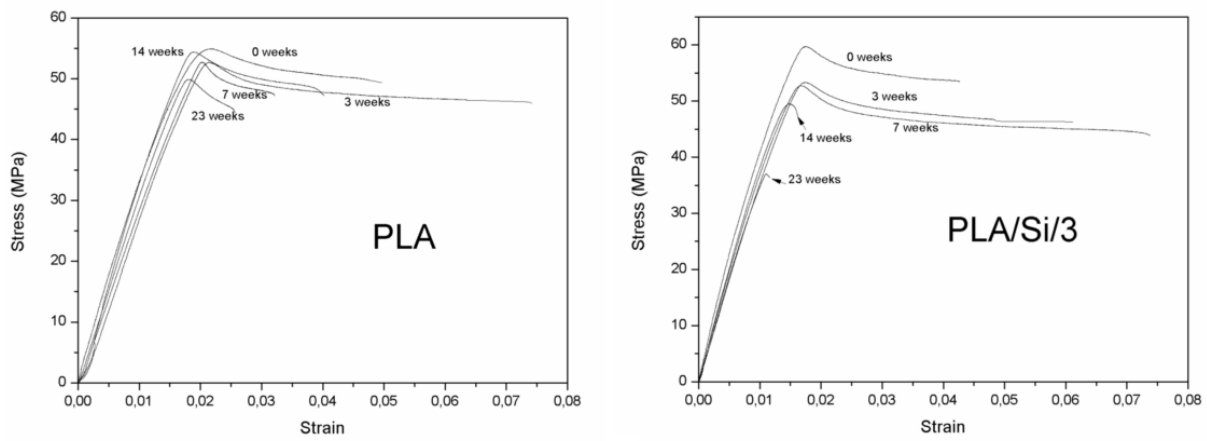

Figure 2. Tensile stress-strain curves for PLA and PLA/Si/3 at various aging conditions.

2.3 Size Exclusion Chromatography (SEC) and Thermogravimetric Analysis (TGA) results

The degradation of PLA matrix has been tested by examining the molecular weight distribution after exposure to the identified aging conditions, for different time periods. The degradation rate was quantified in terms of the average hydrolytic degradation rate constant (k_t). The (k_t) values were evaluated assuming an exponential decrease of number average molecular weight M_n using the following equation [9]:

$$\ln M_n(t_2)=\ln M_n(t_1)-k_t t \quad (1)$$

where $M_n(t_2)$ and $M_n(t_1)$ are the M_n values at the hydrolytic degradation times of t_2 and t_1, respectively. In Fig.3, the molecular weight changes are plotted logarithmically with varying the aging time. In the same plot, analogous results for PLA, degraded under different conditions [9] are depicted for comparison. Following Fig. 3, an average value $\bar{k}_t$ for the hydrolytic degradation rate has been calculated. The estimated $\bar{k}_t$ values for the different time intervals were were 3.73×10^{-4}, 2.96×10^{-3} and 20×10^{-3} days^{-1} at 20, 40 and 50 ˚C, and 80%RH respectively. The sample immersed in the buffer solution at 37 ˚C had an average degradation rate equal to 4.9 x10^{-3} days^{-1}, for a similar time period of aging. The results showed that the degradation rate was higher at the beginning (first 60 days) for every temperature and decreased significantly after 30 days. This finding was in agreement with previous results [1]. Regarding the aging temperature effect, the degradation process was very slow at temperatures equal or below 40 ˚C, but the speed was greatly enhanced at 50 ˚C. As far as TGA results is concerned, it has been found following Figure 4, that the thermal stability of PLA and PLA/Si/5 nanocomposite remains almost unaffected with aging time, while it is reduced, shifted towards lower temperatures, for PLA/Si/2 and PLA/Si/3. This effect denotes that the good quality dispersion of silica at those samples, as postulated by Scanning Electron

Microscopy (not presented here), increases the interfacial region, which is more sensitive to the aging conditions. The formation of large agglomerates in PLA/Si/5 does not have the same effect.

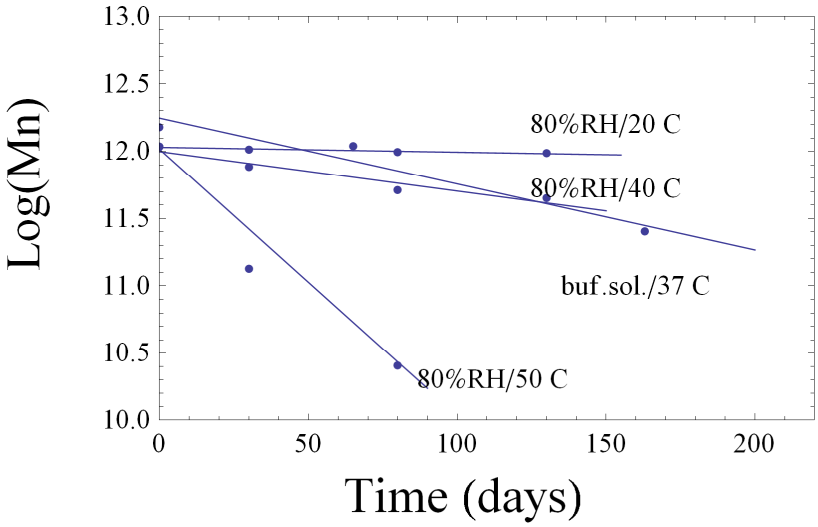

Figure 3. PLA molecular weight variation versus time at various aging conditions.

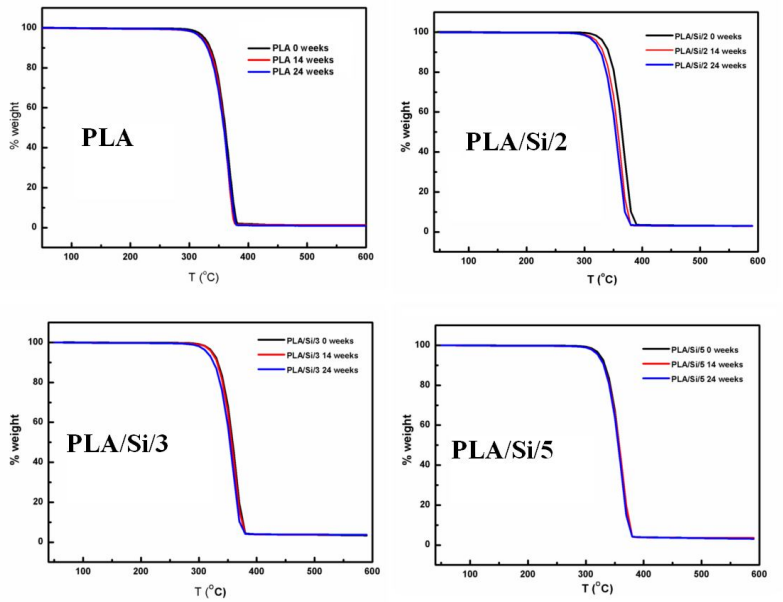

Figure 4. TGA curves for PLA and PLA/Si nanocomposites at various aging times.

3. Micromechanics modeling of elastic stiffness tensor

The elastic stiffness tensor of the nanocomposites under examination has been modeled following a previously introduced micromechanical analysis [10], where the randomly located nanoparticles are coated by an interphase layer, consisting the so-called effective particle. The elastic stiffness tensor of the nanocomposite is thus given by:

$$\overline{\mathbf{C}} = \mathbf{C}^{\mathbf{0}} \bullet \left[\mathbf{I} - \Phi^{\Sigma}\mathbf{T}^{\Sigma} \bullet \left(\Phi^{\Sigma}\mathbf{S} \bullet \mathbf{T}^{\Sigma} + \mathbf{I}\right)^{-1}\right] \qquad (2)$$

Where $\mathbf{C}^{\mathbf{0}}$ is the matrix stiffness tensor, $\mathbf{I}$ the identity tensor, Φ^{Σ} the effective particle volume fraction, $\mathbf{S}$ is the Eshelby tensor, for an isotropic spherical particle and $\mathbf{T}^{\Sigma}$ is a tensor

expressed by **S, C^0** and **C^I,** the elastic stiffness tensors of the interphase. According to the geometry of the particle surrounded by the interphase (Figure 5), the effect of the nanoparticle size can be explicitly introduced on the elastic stiffness tensor, by expressing the quantity Φ^{Σ} as $\Phi^{\Sigma} = \Phi^{P}\left(1+\frac{e}{r_p}\right)^3$ where Φ^P is the particle volume fraction, e is the interphase thickness and r_p is the nanoparticle radius. Following the above equations, the elastic stiffness tensor $\overline{\mathbf{C}}$ can be evaluated, with required parameters the elastic properties of interphase, and consequently the tensile modulus E_c of the composite can be calculated. Poisson's ratio of both matrix materials was taken equal to v_0=0.36. The modulus of silica nanoparticles was taken equal to 72 GPa, and the Poisson's ratio 0.17. The interphase E_i modulus was varied between between matrix and silica nanoparticles' moduli. In Figure 6, the effect of interphase modulus E_i on the normalized modulus $E_n=E_c/E_m$, is demonstrated, with varying the ratio e/r_p, representatively for a constant nanofiller volume fraction Φ^P=3.2% and PLA matrix. A higher enhancement is obtained when interphase thickness is increased in respect to particle radius. Moreover, for the same ratio e/r_p the enhancement is affected up to a certain value of E_i and hereafter, no significant effect is obtained. In the same Figure, the finite element (FE) analysis results are also shown for comparison. In Figure 6, the normalized modulus with varying particle volume fraction Φ^p is also shown at various values of e/r_p , together with the experimental points, and the crucial effect of interphase thickness is apparent. The interphase modulus was taken equal to 35 GPa. Parallel to this analysis, following the expression of Φ^{Σ}, it is assumed that, what actually is distributed is the ratio $r_p/(r_p+e)$. It is further assumed that this ratio obeys a normal Gaussian distribution, determined by a mean value m and a standard deviation s, and consequently the average value $<r_p/(r_p+e)>$ can be evaluated, by treating the tensile data of Table I. These average values were 1.5, 1.32 and 0.9 for PLA/Si/2, PLA/Si/3 and PLA/Si/5 correspondingly, close to the analytically calculated ones. In all cases, the interphase thickness is higher than the particle radius with the exception of PLA/Si/5, which exhibits a peculiar behavior, since the reinforcement at this content was not the expectable one. It is also extracted that in order to have the same reinforcing effect, with increasing the effective particle radius, the interphase thickness needs to be accordingly increased, hence it is extracted that most part of the effective inclusion is interphase like, and the effective particle content is higher that the initial nanofiller loading.

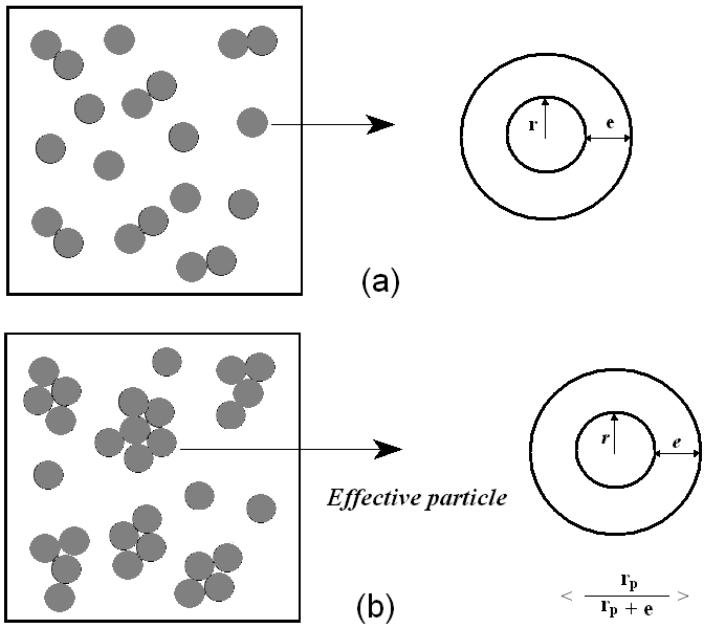

Figure 5. a) Schematic presentation of a nanocomposite material containing spherical particles (left) and a spherical nanoparticle surrounded by the interphase (right). b) Schematic presentation of a nanocomposite material consisted of a distribution of effective particles (left) and an effective particle with average dimensions (right).

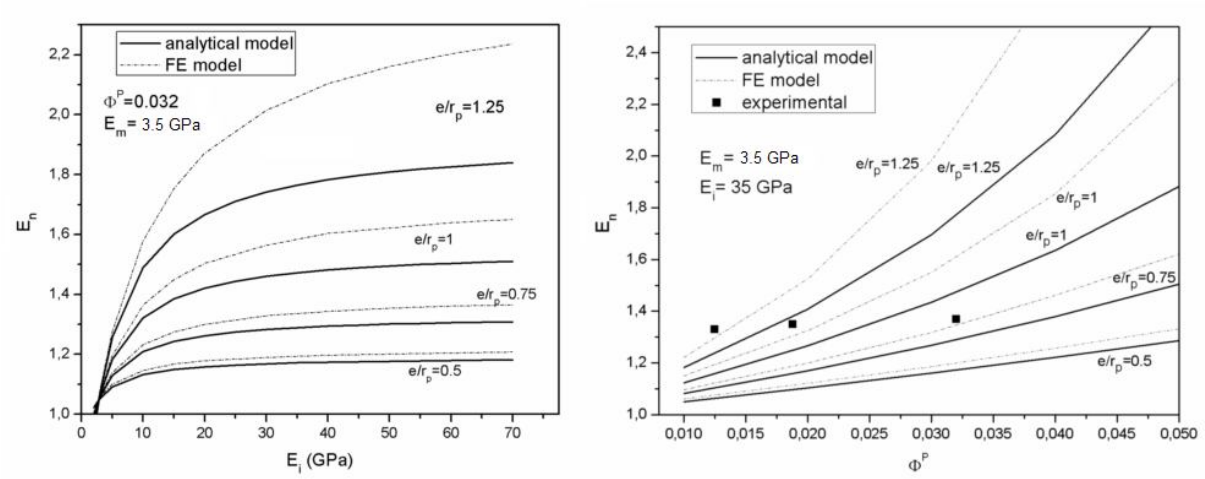

Figure 6. a) Analytical and FE results for normalized modulus with varying interphase modulus at a constant particle volume fraction for PLA matrix (left). b) Normalized modulus with varying particle volume fraction at a constant interphase modulus, for various e/r_p values for PLA matrix (right).

4. Conclusions

The thermomechanical properties of PLA and PLA/Si nanocomposites were extensively studied. The elastic modulus increment of nanocomposites was simulated with a micromechanical model, developed in previous works, where the concept of the effective particle, i.e. nanoparticle surrounded by the interphase region, is considered. Regarding the materials degradation under the specific aging conditions examined, it was found that silica nanoparticles accelerate degradation. A matter of importance has been proved to be the crystallization behavior in PLA and the way it is affected by the presence of nanofillers during

degradation procedure. Values of 44% crystallinity increment were reported for PLA/Si nanocomposites. Therefore, silica is an effective nucleating agent, and promotes crystallization of PLA matrix during hydrolytic degradation.

Acknowledgement

This research has been co-financed by the European Union (European Social Fund – ESF) and Greek national funds through the Operational Program "Education and Lifelong Learning, Research Funding Program Aristeia (E.K.).

References

[1] F. Signori, M-B. Coltelli and S. Bronco. Thermal degradation of poly(lactic acid) (PLA) and poly(butylene adipate-co-terephthalate) (PBAT) and their blends upon melt processing. *Polym Degrad Stab*, 94(1): 74-82, 2009.

[2] S. K. Saha and H. Tsuji. Effects of molecular weight and small amounts of D-lactide units on hydrolytic degradation of poly(L-lactic acid)s. *Polym Degrad Stab*, 91(8):1665-1673,2006.

[3] K. Fukushima, C. Abbate, D. Tabuani, M. Gennari and G. Camino. Biodegradation of poly(lactic acid) and its nanocomposites. *Polym Degrad Stab*, 94(10): 1646-1655, 2009.

[4] E. Kontou, P. Georgiopoulos and M. Niaounakis. The Role of Nanofillers on the degradation behavior of Polylactic Acid. *Polymer Composites*, 33(2): 282-294, 2012.

[5] X. Zhang, M. Espiritu, A. Bilyk and L. Kurniawan. Morphological behavior of poly(lactic acid) during hydrolytic degradation. *Polym Degrad Stab*, 93(10): 1964-1970, 2008.

[6] H. Chen, Y. Wang, J. Chen, J. Yang, N. Zhang, T. Huang and Y. Wang. Hydrolytic degradation behavior of poly(L-lactide)/SiO2 composite. *Polym Degrad Stab*, 98(12): 2672-2679, 2013.

[7] M. Niaounakis, E. Kontou and M. Xanthis. Effects of Aging on the thermomechanical properties of Poly(lactic Acid). *J Appl Pol Sci*, 119(1): 472-481, 2011.

[8] K. Fukushima, D. Tabuani , M. Dottori, I. Armentano, J. M. Kenny and G. Camino. Effect of temperature and nanoparticle type on hydrolytic degradation of poly(lactic acid) nanocomposites. *Polym Degrad Stab*, 96(12): 2120-2129, 2011.

[9] HM. Chen, WB. Zhang, XC. Du, JH Yang, N. Zhang, T. Huang and Y. Wang. Crystallization kinetics and melting behaviors of poly(L-lactide)-graphene oxides composites. *Thermochim Acta*, 566(1):57-70, 2013.

[10] S. Boutaleb, F. Zairi, A. Mesbah, M. Nait-Abdelaziz, JM. Gloaguen, T. Boukharouba and JM. Lefebvre. Micromechanics-based modeling of stiffness and yield stress for silica/polymer nanocomposites. *Int J Solids Struct*, 46(7,8):1716-1726, 2009.